PROCEEDINGS OF SCIENCE

PIC simulations of SNRs shocks with a turbulent upstream medium

Karol Fulat,[a,*] **Artem Bohdan,**[b,c] **Gabriel Torralba Paz,**[d] **Michelle Tsirou**[e] **and Martin Pohl**[a,e]

[a] *Institute of Physics and Astronomy, University of Potsdam, D-14476 Potsdam, Germany*
[b] *Max-Planck-Institut für Plasmaphysik, Boltzmannstr. 2, DE-85748 Garching, Germany*
[c] *Excellence Cluster ORIGINS, Boltzmannstr. 2, DE-85748 Garching, Germany*
[d] *Institute of Nuclear Physics PAN, Radzikowskiego 152, 31-342, Krakow, Poland*
[e] *Deutsches Elektronen-Synchrotron DESY, Platanenallee 6, 15738 Zeuthen, Germany*

E-mail: karol.fulat@uni-potsdam.de

Investigating shock wave properties in supernova remnants (SNRs) is of major importance in understanding the origin and acceleration of cosmic rays. For Diffusive Shock Acceleration electrons must have a highly suprathermal energy, implying a need for very efficient pre-acceleration. Most published studies consider a homogenous upstream medium, which is an unrealistic assumption for astrophysical environments. Using 2D3V particle-in-cell simulations, we investigate electron acceleration and heating processes at high Mach-number shocks with a turbulent upstream medium. For this purpose slabs of plasma with compressive turbulence are separately simulated and then inserted into shock simulations, which requires matching of plasma slabs at the interface. Using a novel technique of matching electromagnetic fields and currents, we perform simulations of perpendicular shocks setting different intensities of density fluctuations ($\lesssim 10\%$) in the upstream. We explore the impact of the fluctuations on electron heating, the dynamics of upstream electrons, and the driving of plasma instabilities. Our results indicate that while the presence of the turbulence enhances variations in the upstream magnetic field, their levels remain too low to influence significantly the behavior of electrons at perpendicular shocks. We extend our investigations to oblique shocks with a turbulent upstream medium, and discuss our latest results.

38th International Cosmic Ray Conference (ICRC2023)
26 July - 3 August, 2023
Nagoya, Japan

*Speaker

PoS(ICRC2023)286

1. Introduction

Understanding the acceleration of particles at shock waves is a crucial challenge for astrophysics and space physics. Although diffusive shock acceleration (DSA; [1]) is considered to be the fundamental acceleration mechanism, it has limitations in describing the behavior observed at interplanetary shocks [2]. An important aspect that still remains poorly understood is the influence of pre-existing upstream turbulence on particle acceleration , see e.g. [3]. Turbulence exists widely throughout astrophysical environments, so it becomes essential to investigate its interplay with shock waves. Another critical issue regarding the DSA theory is that thermal electrons do not satisfy the primary condition of the process. Larmor radii of these particles are significantly smaller than the width of the shock, so they need to be pre-accelerated before undergoing the main acceleration. This is known as the electron injection problem.

This study focuses specifically on shocks in supernova remnants (SNRs), which are thought to be possible candidates for the galactic cosmic rays production. These non-relativistic, collisionless shocks are formed when supernova ejecta interact with the surrounding medium, which is turbulent. They propagate at high velocities of about 1,000 - 10,000 km/s, with sonic and Alfvénic Mach numbers in the range $M_S, M_A \gtrsim 20$. In previous studies of electron acceleration at shocks in SNRs the upstream medium was assumed to be initially homogeneous. This means that all turbulence ahead of the shock wave is driven by shock-reflected particles. It is necessary to confront previous results with new ones that consider pre-existing fluctuations, which are believed to exist in SNR environments.

To properly describe the physics at electron kinetic scales particle-in-cell (PIC) simulations are required. This approach allows to study plasmas from first principles and it is commonly employed to examine shocks in various astrophysical environments [4]. By means of PIC simulations, many studies investigated perpendicular shocks ($\theta_{\rm Bn} = 90^\circ$), and recently the oblique ones ($\theta_{\rm Bn} \approx 50^\circ - 75^\circ$) [5–10], where $\theta_{\rm Bn}$ is the angle between the external magnetic field and the shock normal. Here we investigate the effect of pre-existing turbulence on electron acceleration at non-relativistic high-Mach-number shocks in electron-ion plasma using a novel technique. We focus mainly on well-studied perpendicular shocks, but we also discuss preliminary results from oblique shock simulations.

2. Methods

We perform kinetic simulations using the MPI-parallelized code THATMPI [7, 11] in 2D3V configuration: the 2-spatial and all 3 velocity components of individual particles are tracked. Furthermore, we use a reduced ion-electron mass ratio $m_i/m_e = 100$. This approach allows us to save computational resources when compared to running full 3D simulations and those with the realistic mass ratio, while still maintaining reasonable accuracy in capturing the physics of shock waves.

An incoming plasma beam moves with velocity $v_0 = 0.2c$ in the negative x-direction. It is reflected off a conducting wall at $x = 0$, creating a shock, which propagates in the positive x-direction. The Mach numbers of such shock are roughly equal to $M_S, M_A \sim 30$. This setup determines the downstream frame as the reference frame of the simulation. For this reason, it is

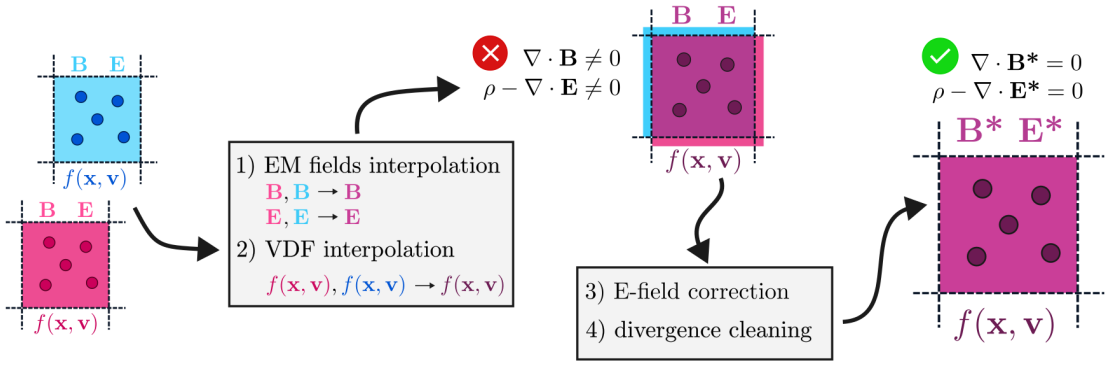

Figure 1: The matching procedure of two arbitrary plasma slabs presented for one grid cell.

Run	H	T1	T2	H′	T′
$\delta n/n$ [%]	-	3.5	10	-	15
θ_{Bn} [°]	90	90	90	60	60
M_S/M_A	36/32	36/32	36/32	33/30	33/30

Table 1: The density fluctuation amplitudes and the obliquity angles for all runs. All simulations have the same plasma beta $\beta \approx 1$.

necessary to continuously replenish the upstream plasma flowing towards the shock. In contrast to simulations with a homogeneous upstream medium, where plasma can be added in a thin layer, a plasma carrying pre-existing fluctuations has to be established separately and then injected into the shock simulation.

Slabs of compressive turbulence are pre-fabricated in dedicated simulations with periodic boundaries. The simulation box is a square, the size of which corresponds to the width of the shock simulation into which they are to be injected. In the pre-fabrication stage, density fluctuations are obtained by superposition of wave-like disturbances of the local bulk velocity. Following an initial period of rapid evolution, the magnitude of the density fluctuations is stable for at least two ion Larmor times. The magnetic field fluctuations evolve self-consistently, but are weaker than the density fluctuations. Furthermore, the intensity and spectrum of the fluctuations do not vary significantly during the shock simulation.

Damping at kinetic scales converts wave energy into plasma heat. It is therefore necessary to start the pre-fabrication with lower initial temperatures and to ensure that the temperature upon insertion into the shock simulation matches the desired sonic Mach number. This limits the achievable level of density fluctuations, from our empirical tests the fluctuation amplitude cannot be much larger than $\delta n/n \sim 10\%$, where the root-mean-square of the particle density fluctuations (on the scale of a quarter of the ion skin length) is denoted by δn, and n represents the mean density. This number roughly corresponds to measurements in the local interstellar medium [13]. The pre-fabricated plasma slabs must be inserted into our shock simulation frequently, to ensure computational efficiency and to maintain a consistent evolution state of the turbulence. It is necessary to carefully match each new slab with the adjacent plasma to avoid any unwanted artifacts or transients. Our novel matching procedure is shown in Fig. 1.

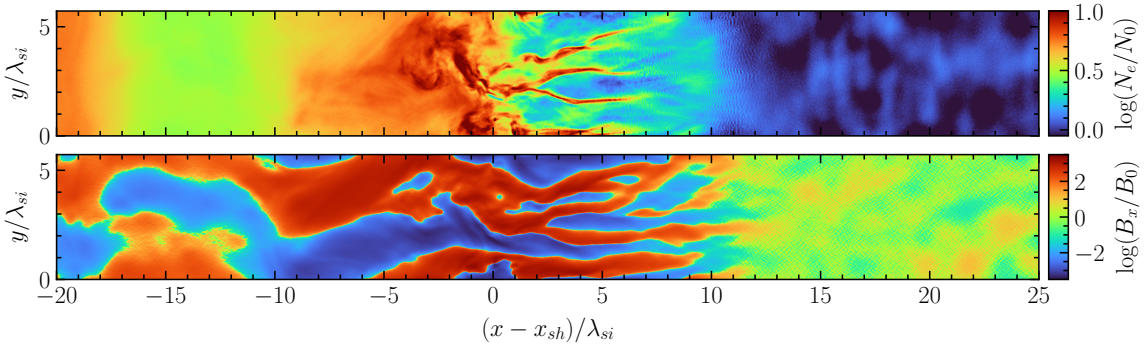

Figure 2: Maps of the electron number density (*top*) and the x-component of the magnetic field (*middle*) at a perpendicular shock with pre-existing turbulence (run T2) at approximately ten ion Larmor times. The scaling of the B_x/B_0 is logarithmic and sign-preserving: $\mathrm{sgn}(B_x) \cdot [2 + \log\{\max(10^{-2}, |B_x|/B_0)\}]$.

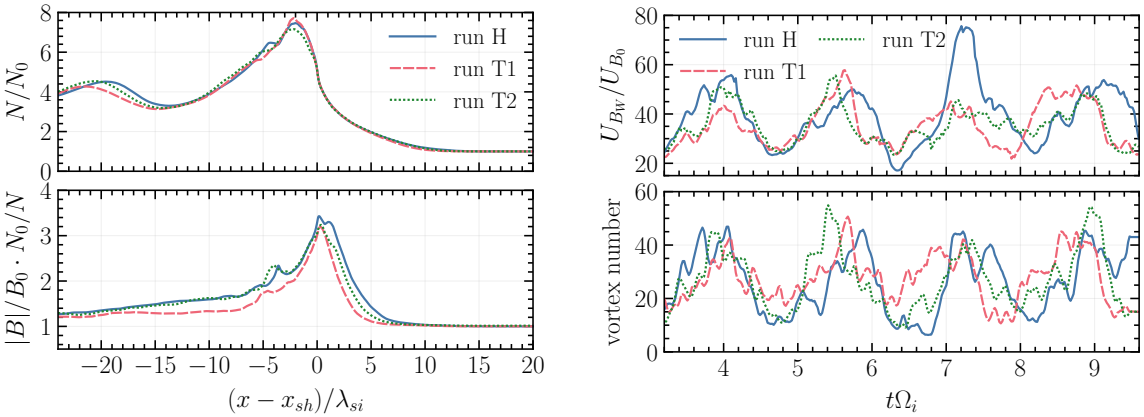

Figure 3: Left: the ion number density profile averaged over the y-direction (*top*) and the ratio of the magnetic-field strength to the density (*bottom*). Right: the evolution of the energy density of the Weibel-generated magnetic field (*top*) and the evolution of the number of the magnetic vortices (*bottom*).

3. Results

Here we examine the influence of compressive pre-existing turbulence on high-Mach-number shocks. All the simulations we have performed are outlined in Table 2. Among these simulations, three pertain to perpendicular shocks: one with a homogeneous upstream medium (H), while the other two consider different amplitudes of density fluctuations, $\delta n/n = 3.5\%$ (T1) and $\delta n/n = 10\%$ (T2). Additionally, we also briefly discuss preliminary results from oblique shock simulations, marked with the prime symbol.

3.1 Perpendicular shocks

The reflection of upstream ions, which in the case of a perpendicular shock is an ordinary gyration in the shock-compressed magnetic field, causes the formation of the following distinct regions: the foot, the ramp, and the overshoot-undershoot structure downstream of the shock. The structure of a perpendicular shock propagating in turbulent medium is presented in Fig. 2. The upstream plasma is located at $x - x_{sh} \gtrsim 12\lambda_{si}$ and it carries density fluctuations (*top* panel) together

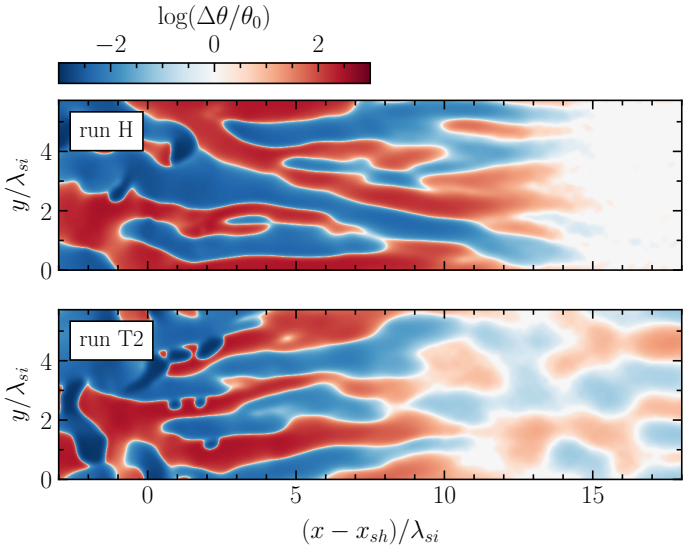

Figure 4: Maps of the difference between the local obliquity angle and the inclination angle of the external magnetic field for the runs H and T2, respectively, at roughly nine ion Larmor times. The maps are presented in logarithmic and sign-preserving scale: $\mathrm{sgn}(\Delta\theta) \cdot [2.5 + \log\{\max(10^{-2.5}, |\Delta\theta|/\theta_0)\}]$.

with weaker fluctuations of the magnetic field (*bottom* panel). The next characteristic region is the shock foot at $(10 - 12)\lambda_{si}$ ahead of the shock front. It contains electrostatic waves generated by the Buneman instability, represented by small-scale features in the *top* panel. The foot region is followed by the ramp extending towards the overshoot at $x - x_{sh} \approx -1\lambda_{si}$. The electromagnetic Weibel instability operates there, creating filamentary structures visible in both the density and the magnetic field maps. The transition to the shock downstream is marked by an overshoot-undershoot pattern about $10\lambda_{si}$ behind the shock front.

The ion-density profiles and the magnetic field strength for all perpendicular runs are compared in Fig. 3 (*left*). The upstream turbulence, regardless of its intensity, does not affect either the characteristic shock structure or the compression ratio. There are none of the shock distortions observed in previous kinetic simulations [12]. To remove the effect of compression, the magnitude of the magnetic field is normalized by the particle density. It reaches the same maximum value at the overshoot for all simulations, suggesting that the amplification of the magnetic field is not modified by pre-existing density fluctuations with amplitudes below 10%.

The electrostatic Buneman instability in the shock foot and the electromagnetic Weibel instability at the shock ramp are the two main instabilities that affect both the electron dynamics and the structure of perpendicular shocks. The Buneman waves play an important role in the heating of electrons and their acceleration via shock surfing acceleration. They are driven due to the interaction between shock-reflected ions and incoming electrons. The reflection of the ions is non-stationary, which means that the waves are driven in a quasi-periodic manner. To compare the wave activity in different simulations, we average the electrostatic energy density in the shock foot over multiple ion reflection cycles. The measured values for all runs are comparable: $1.6 \cdot 10^{-3} n_e m_e c^2$ for run H, $1.1 \cdot 10^{-3} n_e m_e c^2$ for run T1 and $1.3 \cdot 10^{-3} n_e m_e c^2$ for run T2.

The interaction of the incoming ions with those reflected at the shock front leads to the growth of the Weibel instability. This instability is responsible for the amplification of the magnetic field, as well as the modification of its topology. To compare the strength of the instability in different simulations, the evolution of the energy density of the Weibel-generated magnetic field

is followed, see Fig. 3 (*right*). The Weibel-generated field is defined as the magnetic field in the region $-5\lambda_{si} < x - x_{sh} < 15\lambda_{si}$, with the effect of compression removed. The non-stationary ion reflection at the shock front causes the cycle-to-cycle variations in the quasi-periodic behavior. In addition, the Weibel-created filaments may become tearing-mode unstable and eventually decay through magnetic reconnection, creating magnetic vortices. Fig. 3 (*right*) compares the number of vortices among all runs. On average, the evolution of the energy density and vortex number is analogous for all simulations, suggesting that the instability is not affected by the pre-existing turbulence.

Particle reflection at a shock may be affected by local changes in the shock obliquity angle. These can result from variations of the magnetic field ahead of the shock front. Fig. 4 shows maps of the difference between the local obliquity angle and the inclination angle of the external magnetic field: $\Delta\theta = \theta - \theta_0$, where θ_0 represent the obliquity angles listed in Table 2. In the region $x \geq 13\lambda_{si}$ for run T2 (*bottom* panel) the variations of the obliquity angle correspond to the magnetic field fluctuations carried by the pre-existing turbulence. The amplitudes of $\Delta\theta$ in this region are higher than for run H (*top* panel), but further to the shock the Weibel instability dominates the structure of the field.

Particle interactions, such as shock-surfing acceleration and magnetic reconnection, determine the shape of the electron energy spectra in the downstream, as well as their temperature. The spectral shapes and the temperature values measured in our simulations are similar for all runs. It is consistent with the analysis of the Buneman and the Weibel instabilities, which shows no significant influence of the pre-existing density fluctuations on their strength.

4. Oblique shocks

In this section we present preliminary results from simulations of oblique shocks (see primed runs in Table 2). To investigate the influence of pre-existing density fluctuations, we used similar parameters to ones in [10]. The magnetic field has an out-of-plane configuration: $\mathbf{B}_0 = B_0 \cdot (\cos\theta_{\rm Bn}, \cos\theta_{\rm Bn}\phi, \sin\theta_{\rm Bn}\sin\phi)$, where $\theta_{\rm Bn} = 60^\circ$ and $\phi = 90^\circ$.

In perpendicular shocks particles are closely confined to the shock front by the inclination of the external magnetic field. Contrarily, at shock with angles in the range of $\theta_{\rm Bn} \approx 50^\circ - 75^\circ$ some energetic electrons escape the shock and travel further to upstream. Therefore, the shock foot is replaced by an extended region called the foreshock, where reflected particles drive instabilities. For run with pre-existing turbulence the foreshock is significantly shorter, which implies that the dynamic of the shock-reflected electrons is modified.

Fig. 5 compares the electron momentum distributions in the foreshock region for runs H′ (panels a – c) and T′ panels (d – f), at seven ion Larmor times. Two electron populations can be distinguished in this region: the incoming cold beam and the shock-reflected particles. The first one is represented by the the bright dot at $(p_x, p_y, p_z)/mc = (0.2, 0, 0)$. The signal is narrow since the plasma has low temperature. The population of the reflected electrons can be easily recognized in panels b and e: the energized particles follow the external magnetic field lines thus they have positive p_x and p_z components. For run with pre-existing density fluctuations the distributions are wider, which means that the particles have higher temperatures. Moreover, the $p_x - p_y$ distribution for run T′ is significantly less anisotropic.

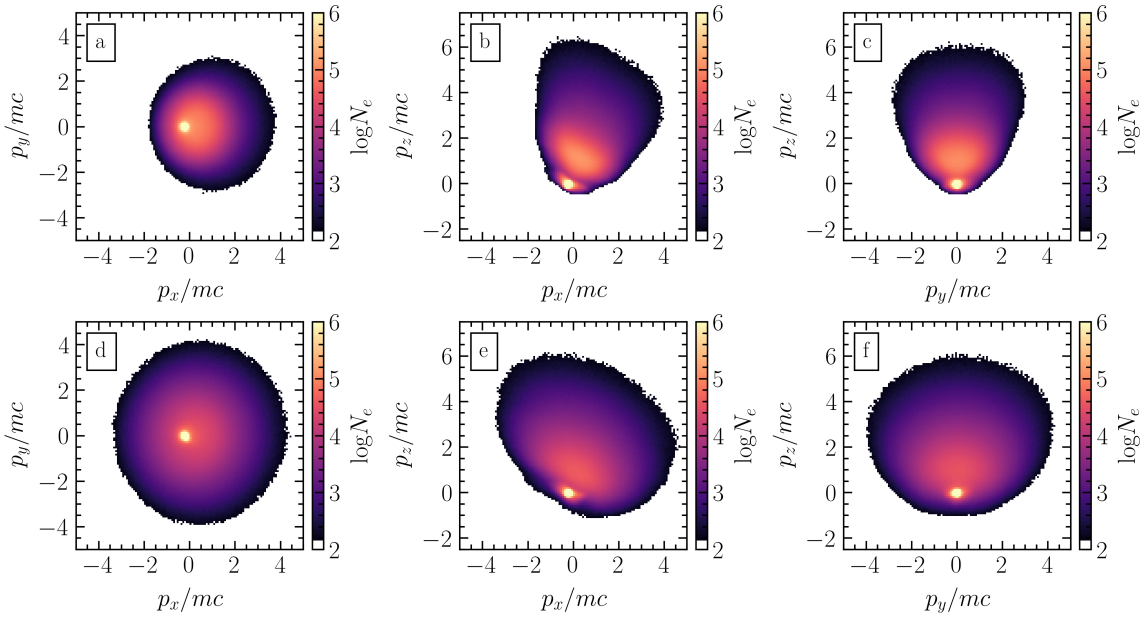

Figure 5: Momentum distribution of electrons in the foreshock region for simulation with a homogeneous upstream medium (run H′, panels a – c) and for simulation with pre-existing turbulence (run T′, panels d – f).

5. Summary and conclusions

Two simulations of a perpendicular high-Mach-number shock with different RMS amplitude of pre-existing density fluctuations were performed: $\delta n/n = 3.5\%$ and $\delta n/n = 10\%$. The impact of the turbulence on the shock physics and the electron dynamics were studied by direct comparison to a simulation with a homogeneous upstream medium. Additionally, preliminary results from oblique shocks propagating in turbulent medium were discussed. The main conclusions are:

1. The achievable level of pre-existing upstream turbulence at kinetic scales is constrained by particle heating. Our empirical tests suggest that, to maintain a sonic Mach number larger than $M_S \gtrsim 30$, the maximum amplitude of the density fluctuations should be at most of the order of $\delta n/n \sim 10\%$ (on the scale of a quarter of the ion skin length).

2. Density fluctuations up to a few λ_{si} and with amplitudes in concordance with in-situ measurements, $\delta n/n \lesssim 10\%$, do not significantly affect the physics of high-Mach-number perpendicular shocks.

3. The properties of the electron foreshock at oblique shocks are affected by pre-existing density fluctuations of amplitude $\delta n/n \lesssim 15\%$. This region becomes shorter and hotter compared to the case with homogeneous medium, which implies that the distribution of the shock-reflected electrons is less anisotropic.

6. Acknowledgments

K. F. and M. P. acknowledge support by DFG through grant PO 1508/10-1. *Energy Partition across collisionless shocks*. A. B. was supported by the German Research Foundation

(DFG) as part of the Excellence Strategy of the federal and state governments - EXC 2094 - 390783311. G. T. P. acknowledge support by Narodowe Centrum Nauki through research project No. 2019/33/B/ST9/02569. This research was supported by the International Space Science Institute (ISSI) in Bern, through ISSI International Team project #520. The numerical simulations were conducted on resources provided by the North-German Supercomputing Alliance (HLRN) under-project bbp00057. We gratefully acknowledge Polish high-performance computing infrastructure PLGrid (HPC Centers: ACK Cyfronet AGH) for providing computer facilities and support within computational grant no. PLG/2022/015967.

References

[1] Bell, A. R., 1978, MNRAS, 182, 147-156.

[2] Lario, D., et al., 2003, AIP conference proceedings, 679, 640-643.

[3] Guo, F., Giacalone, J. and Zhao, L., 2021, Front. astron. space sci., 8.

[4] Pohl, M., Hoshino, M. and Niemiec, J., 2020, Progress in particle and nuclear physics, 111.

[5] Matsumoto, Y., Amano, T., Kato, N. and Hoshino, M., 2015, Science, 347.

[6] Matsumoto, Y., Amano, T., Kato, T. N., and Hoshino, M., 2017, PRL, 119, 105101.

[7] Bohdan, A., Niemiec, J., Kobzar, O. and Pohl, M., 2017, ApJ, 847, 71.

[8] Bohdan, A., 2023, Plasma physics and controlled fusion, 65.

[9] Morris, P. J., Bohdan, A., Weidl M. S. and Pohl, M., 2022, ApJ, 931.

[10] Morris, P. J., et al., 2023, ApJ, 944

[11] Niemiec, J., Pohl, M., Stroman, T., et al. 2008, ApJ, 684, 1174.

[12] Demidem, C., Nättilä, J. and Veledina, A., 2023, ApJL, 947.

[13] Fraternale, F., et al., 2022, Space Science Reviews, 218.